REPORT No. 289

FORCES ON ELLIPTIC CYLINDERS IN UNIFORM AIR STREAM

By A. F. ZAHM, R. H. SMITH, and F. A. LOUDEN

Aerodynamical Laboratory, Bureau of Construction and Repair
United States Navy

REPORT No. 289

FORCES ON ELLIPTIC CYLINDER IN UNIFORM AIR STREAM

By A. F. Zahm, R. H. Smith, and F. A. Louden

INTRODUCTION

This report presents the results of wind tunnel tests on four elliptic cylinders with various fineness ratios, conducted in the Navy Aerodynamic Laboratory, Washington. The object of the tests was to investigate the characteristics of sections suitable for streamline wire which normally has an elliptic section with a fineness ratio of 4.0; also to learn whether a reduction in fineness ratio would result in improvement; also to determine the pressure distribution on the model of fineness ratio 4.

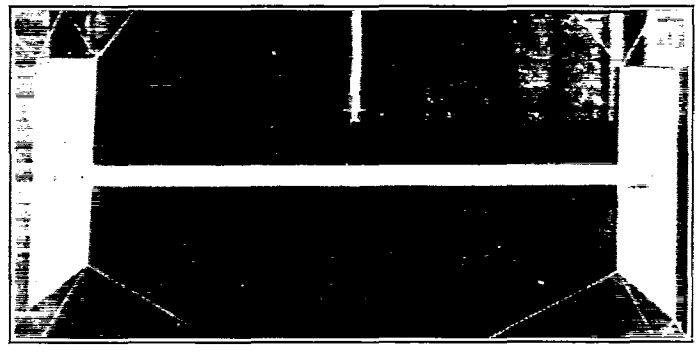

Fig. 1.—Elliptic cylinder 2 by 5 inches mounted with end plates

Four elliptic cylinders with fineness ratios of 2.5, 3.0, 3.5, and 4.0 were made and then tested in the 8 by 8 foot tunnel; first, for cross-wind force, drag, and yawing moment at 30 miles an hour and various angles of yaw; next for drag at 0° pitch and 0° yaw and various wind speeds; then for end effect on the smallest and largest models; and lastly for pressure distribution over the surface of the largest model at 0° pitch and 0° yaw and various wind speeds. In all tests, the length of the model was transverse to the current. The results are given for standard air density, $\rho = .002378$ slug per cubic foot.

This account is a slightly revised form of Report No. 315, prepared for the Bureau of Aeronautics, July 13, 1926, and by it submitted for publication to the National Advisory Committee for Aeronautics. A summary of conclusions is given at the end of the text.

DESCRIPTION OF MODELS

The four elliptic cylinders, the smallest of which is shown in Figure 1, and profiles of which are shown in Figure 10, were each 62 inches long and 2 inches thick; their widths were 5, 6, 7, and 8 inches. The specified offsets are given in Table 1 and for each case can be derived from the equation of an ellipse. All of the cylinders were of laminated pine, varnished, and then verified by application of their construction templates. After the tests, however, a few measurements of offsets taken on the plane table indicated that the models were slightly unsymmetrical. The 2 by 8 inch cylinder had detachable end segments to fill up the space between the floor and ceiling of the tunnel during the pressure distribution test.

In a second test series adjoining end plates, Figure 1, were used to determine the end effect on two of the cylinders. They were made from fairly plane galvanized-iron plate and measured 24 by 24 inches.

In Figure 2 the pressure collector is shown inserted as a center segment in the 2 by 8 inch model. It was made of bronze accurate to 0.001 inch in the offsets. Its dimensions and the location of its 16 holes are given in Figure 3. The pressure leads, one running from a hole in the nose and the other successively from each surface hole, were each connected with ¼-inch tubing which ran lengthwise through the strut to a manometer outside the tunnel.

49296—29——15

METHOD OF TESTING

To measure the forces and yawing moment, each cylinder was mounted, without end plates, at its center on the two-prong fork, Figure 1, extending from the shank of the tri-dimensional balance described in reference 1. The angle of yaw was varied from $-6°$ to $20°$ by $2°$ intervals, the wind speed was held at 30 miles an hour, and the cross-wind force, drag, and yawing moment were simultaneously measured on the cylinder and exposed portion of the holder; then on the holder alone with the cylinder detached but not removed. The difference was taken as the true force or moment component. The precision of such measurements is given in Reference 2. The drag measurements with the cylinders at $0°$ pitch and $0°$ yaw were taken in the same way; the wind speed being varied from 20 to 60 miles an hour by 10 mile intervals.

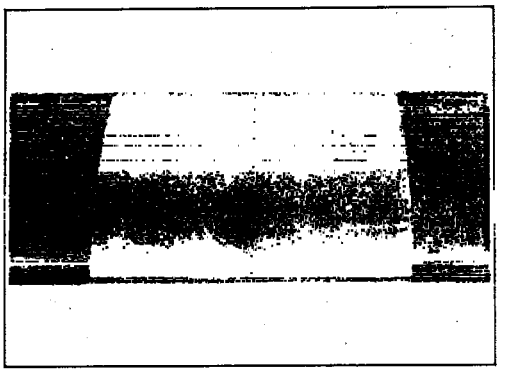

FIG. 2.—Pressure collector inserted in 2 by 8 inch elliptic cylinder

To determine the end effect of the smallest and largest cylinders, the plates were mounted at the ends of the model as shown in Figure 1, and the cross-wind force and drag were measured at intervals of $4°$ yaw. The measurements were repeated without the plates. The percentage difference applied to the original force data gave values for the infinite cylinder.

The pressure distribution measurements were made on the 2 by 8 inch cylinder, which was mounted vertically in the tunnel with extension end segments accurately in line and with the pressure collector inserted in the middle of its span. The difference of pressure between the nose and each of the holes aft of the nose was determined successively. To do this all the surface holes were plugged except one which was joined to one pressure lead, while the nose hole was joined to the other lead. The wind speed was then varied from 20 to 70 miles an hour, by 10 mile intervals, and the differential pressure was measured on an alcohol manometer having a 1 to 10 slope. These measurements could be read in all cases to within 0.005 inch vertical of alcohol. Thus the point pressure could be determined to about one-half of 1 per cent for speeds above 40 miles an hour; to within less than 2 per cent for the lower speeds. The air speed was held constant to within one-half of 1 per cent.

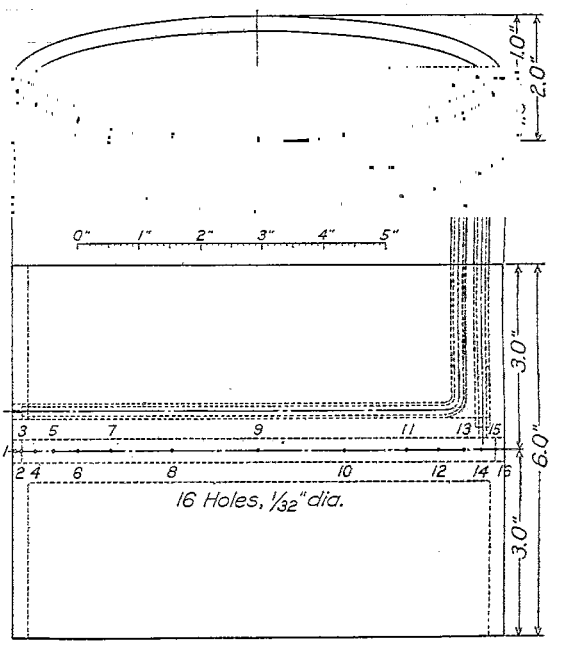

FIG. 3.—Bronze pressure collector for elliptic cylinder 2 by 8 inches, fineness ratio 4

RESULTS OF FORCE AND MOMENT MEASUREMENTS

The cross-wind force and drag on the 62-inch cylinders at various angles of yaw are given in Tables II and III together with their coefficients which are the respective forces divided by $\frac{1}{2}\rho V_1^2$ times the frontal area S, V_1 being feet per second. The coefficients are plotted in Figures 4 and 6.

The cross-wind coefficient [1] increases positively at negative yaw and negatively at positive yaw as the fineness ratio is increased from 2.5 to 4.0. The fact that the force is not zero at zero yaw is probably due to the models being slightly unsymmetrical. The maximum coefficient is -4.28 for the 2 by 8 inch cylinder.

[1] To express these cross-wind coefficients as lift coefficients, multiply them by frontal area/chord-plane area.

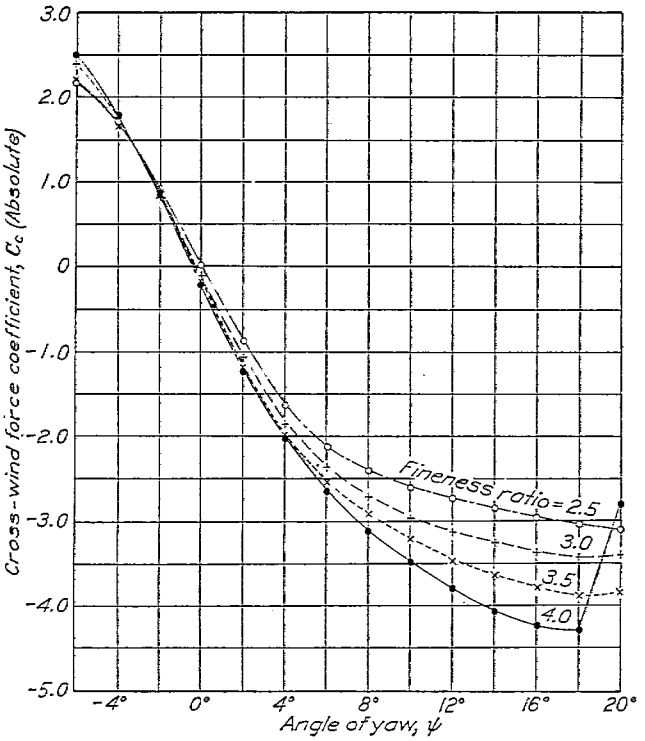

FIG. 4.—Elliptic cylinders of various fineness ratios. Length of cylinder 62 inches, models at 0° pitch, air speed 30 M. P. H.

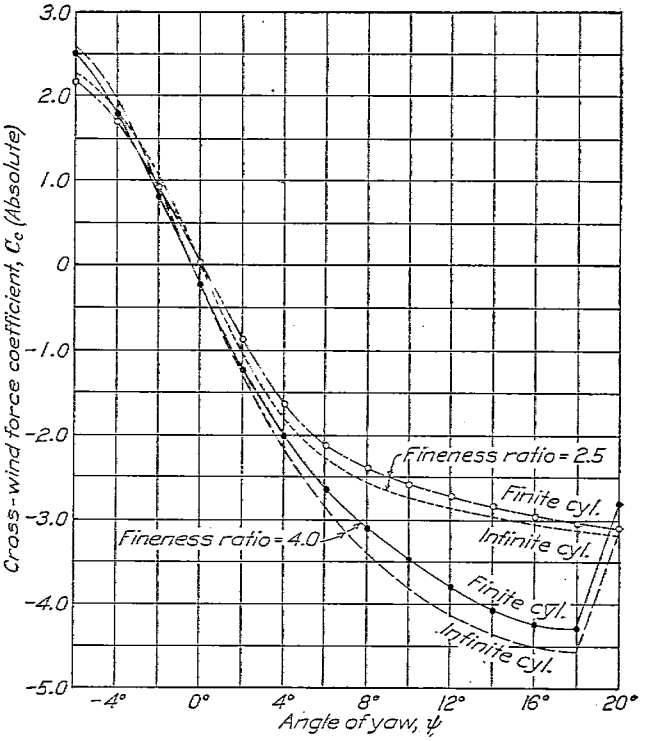

FIG. 5.—Elliptic cylinders of fineness ratios 2.5 and 4. Length of cylinder 62 inches, models at 0° pitch, air speed 30 M. P. H.

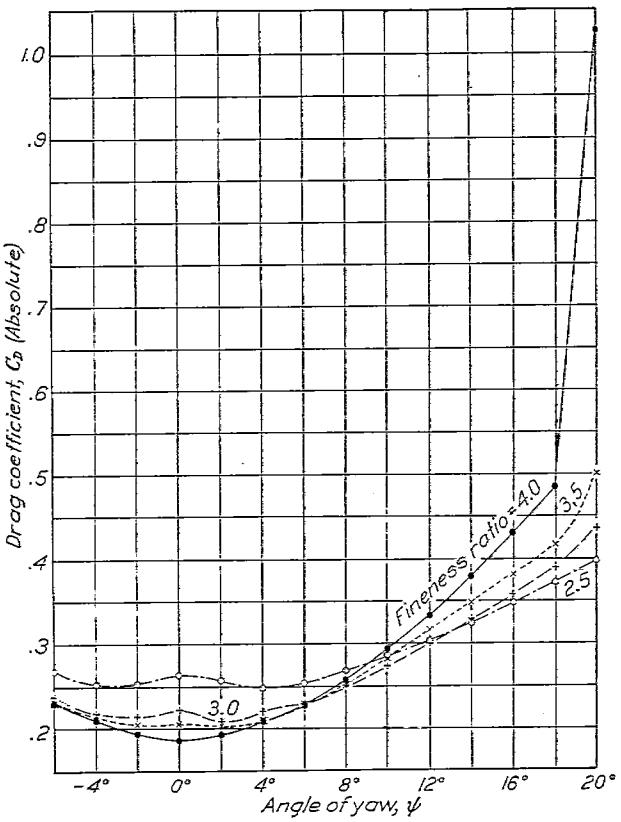

FIG. 6.—Elliptic cylinders of various fineness ratios. Length of cylinder 62 inches, models at 0° pitch, air speed 30 M. P. H.

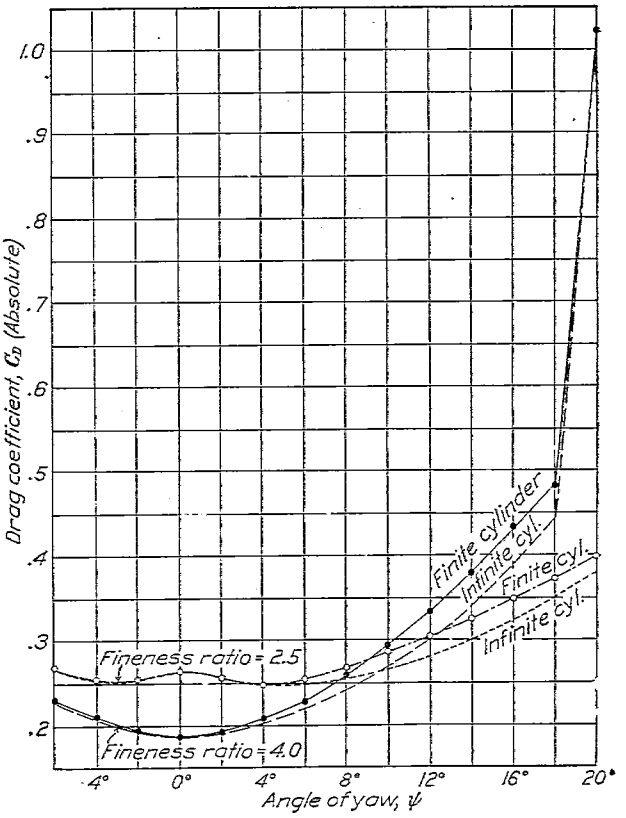

FIG. 7.—Elliptic cylinders of fineness ratios 2.5 and 4. Length of cylinder 62 inches, models at 0° pitch, air speed 30 M. P. H.

The drag coefficient is decreased by increasing the fineness ratio at zero yaw, but the difference is less as the yaw increases and between 4° and 6° the cylinder of fineness ratio 3.5 has a drag coefficient equally as low as the 2 by 8 inch cylinder. From 6° to 13°, the 2 by 6 inch cylinder has the least drag coefficient; beyond 13° yaw, the greater the fineness ratio the greater the drag coefficient.

The yawing moment about the N-axis is presented in Table IV; the resulting lines of force and the center of pressure travel are shown in Figures 9 and 10. As the fineness ratio of the cylinder increases, the center of pressure moves slightly aft.

The ratio of the forces C/D, is given in Table 5 and the graphs are given in Figure 8. The 2 by 8 inch cylinder is superior for angles of yaw up to 16°. C/D max. for this cylinder is -12 at 8° yaw.

Tables VI and VII give the force measurements on the smallest and largest model with and without end plates, the percentage difference and the coefficients for the infinite cylinder; Figures 5 and 7 compare the coefficients of the finite and infinite cylinders. The cross-wind force coefficient is increased positively at negative yaw and negatively at positive yaw when the cylinder becomes endless. The drag coefficient for the infinite cylinder is less than for the finite.

With the cylinders at 0° pitch and yaw, the resistance and corresponding coefficients for various speeds are given in Table VIII and plotted in Figure 11. Here the resistance of the 62-inch cylinder was taken to be substantially the same as for a 62-inch segment of an infinite cylinder, as the increment due to end effect was small and could not be measured. On comparing the four struts, it is seen that at high speeds the drag coefficient is not lowered by increase of fineness ratio; at speeds of 50 and 60 miles an hour, the models with fineness ratios of 3.0 and 3.5 have a lower coefficient than the 2 by 8 inch model.

RESULTS OF PRESSURE DISTRIBUTION MEASUREMENTS

The differential pressure measurements made on the 2 by 8 inch cylinder are presented in Table IX, and their conversion from inches of alcohol on a 1 to 10 slope to vertical inches of water is also given. Table X gives the point pressure at the several holes found by subtracting the differential pressure from the nose pressure. These data are plotted in Figures 12 and 13. Table XI gives the point pressure in terms of the nose pressure.

One sees from Figure 12 that for this strut shape the point pressure at all used speeds decreases from full impact $\frac{1}{2}\rho V^2$ at the nose to zero at a distance of 2.1 per cent of the cylinder width from the nose; the maximum suction occurs at about three-eighths of the width from the leading edge and is equal to about .6 the nose pressure. For speeds of 40 to 70 miles an hour there is another point of zero pressure near the trailing edge and a positive pressure aft of that; for the lower speeds, a slight suction is still evident at the trailing edge. Figure 13 shows that the pressure at each hole varies nearly as the square of the velocity.

The graphs of the faired values of the point pressure, multiplied by $(70/V)^2$ to make them comparable are shown in Figure 14. The integrals of each pressure graph, giving the elements of the pressure drag and the summation of these or the resultant pressure-drag, are given in Table 12 and plotted in Figure 15. With them are shown the total drag and the resultant friction. The order of graphic integration here used to find the force $\int pdy$ over the various portions of the surface of the 1-foot-long center segment of the cylinder is detailed in the diagrams of Figure 17.

It is seen that the downstream push and the upstream suction vary as V^n. The upstream push is zero at low speeds since the pressure did not become positive near the trailing edge of the model at these speeds. The difference between the total downstream and upstream pressure forces, which is the pressure drag, is seen to increase up to a speed of 35 miles an hour and then decrease. The difference between the curves of total drag and pressure drag, giving the frictional drag, varies as V^n where $n=1.97$.

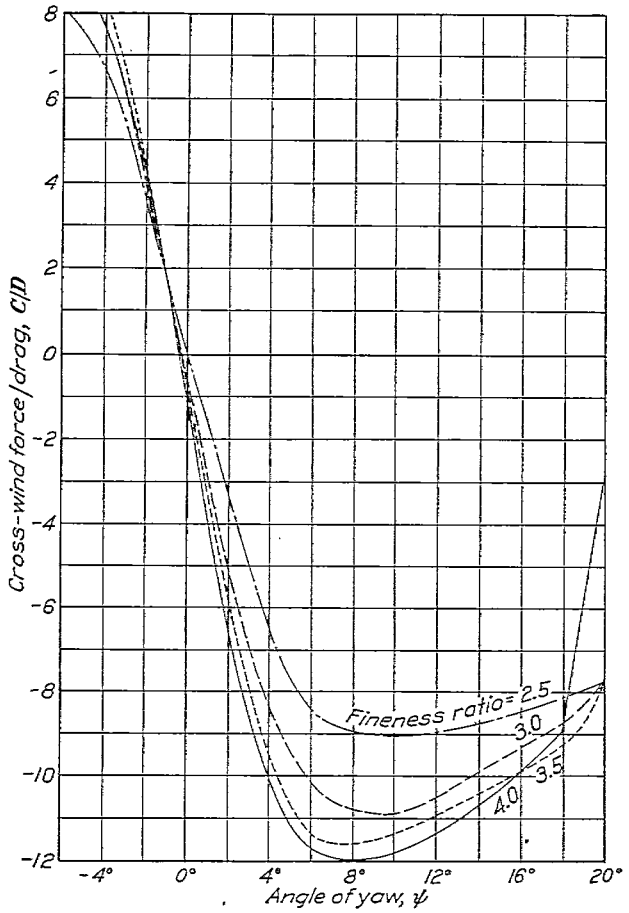

FIG. 8.—Elliptic cylinders of various fineness ratios. Length of cylinder 62 inches, models at 0° pitch, air speed 30 M. P. H.

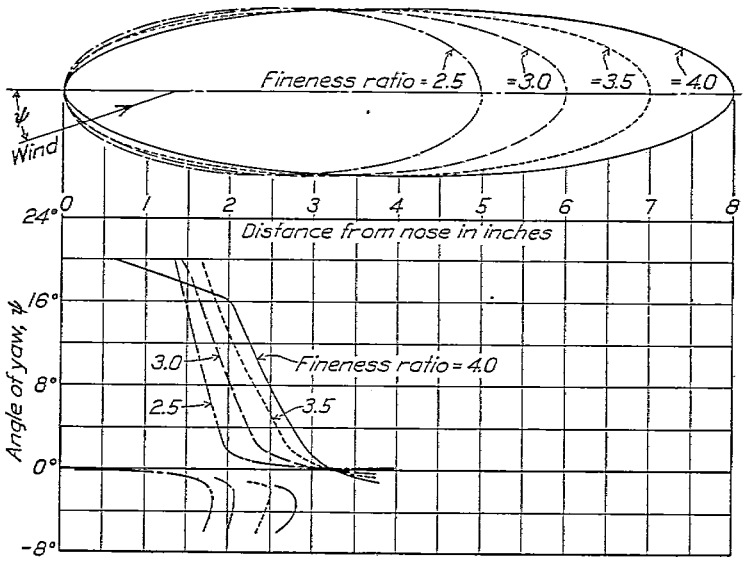

FIG. 10.—Center of pressure at various angles of yaw, of elliptic cylinders of various fineness ratios. Length of cylinder 62 inches, models at 0° pitch, air speed 30 M. P. H.

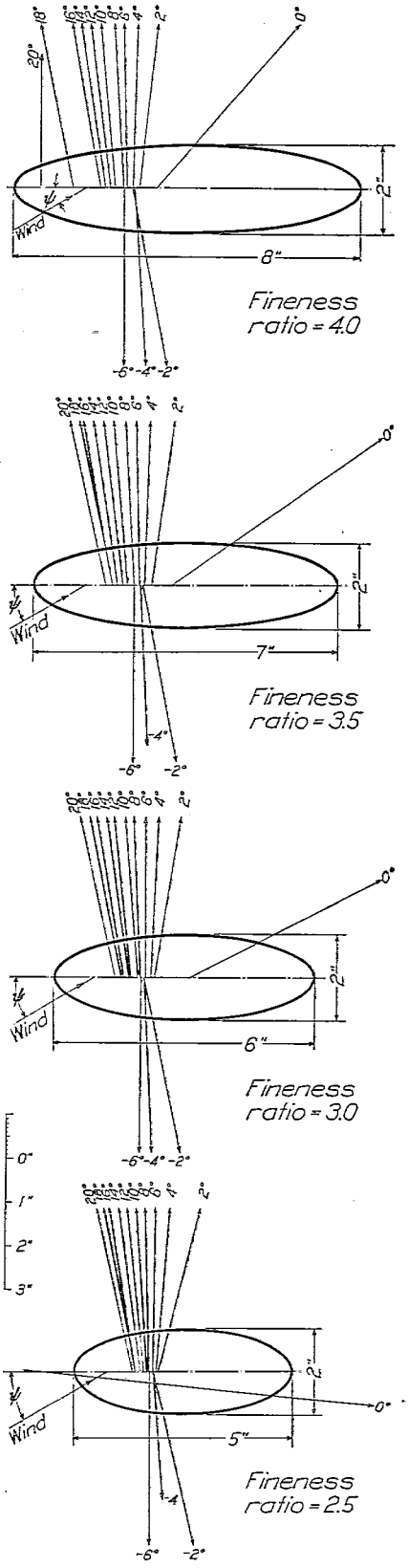

FIG. 9.—Lines of resultant air force at 30 M. P. H. of elliptic cylinders of various fineness ratios. Length of cylinder 62 inches, models yawed at 0° pitch

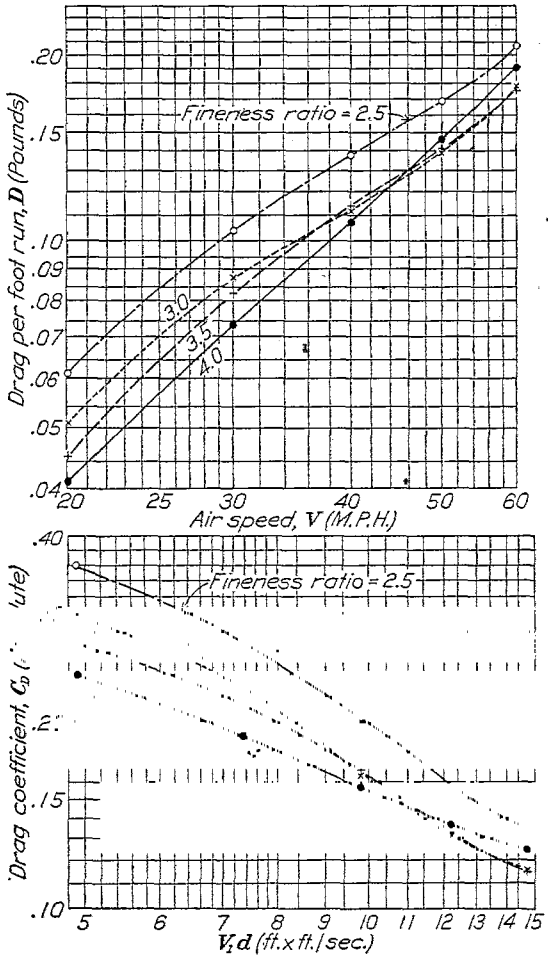

FIG. 11.—Elliptic cylinders at various fineness ratios. Models at 0° pitch and 0° yaw

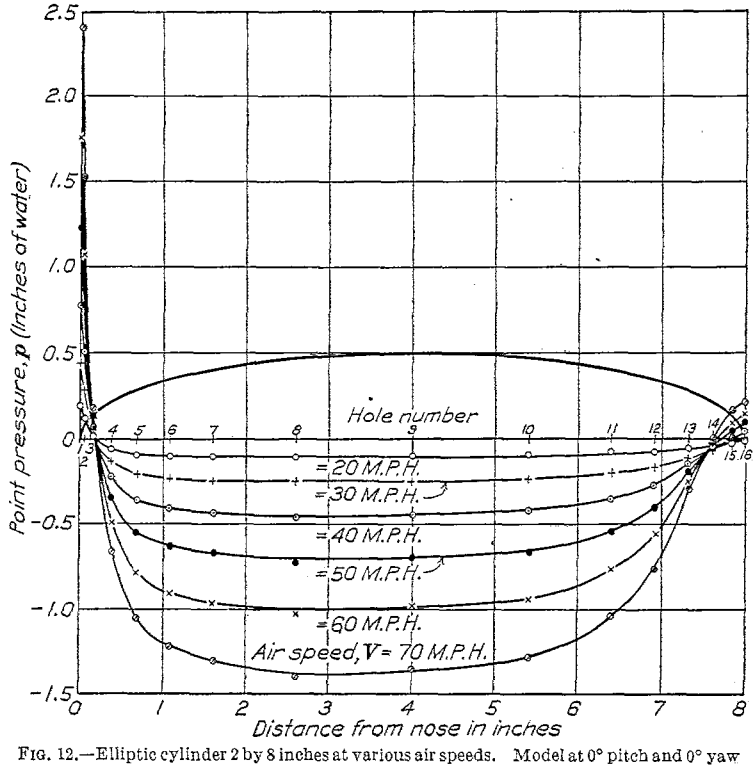

FIG. 12.—Elliptic cylinder 2 by 8 inches at various air speeds. Model at 0° pitch and 0° yaw

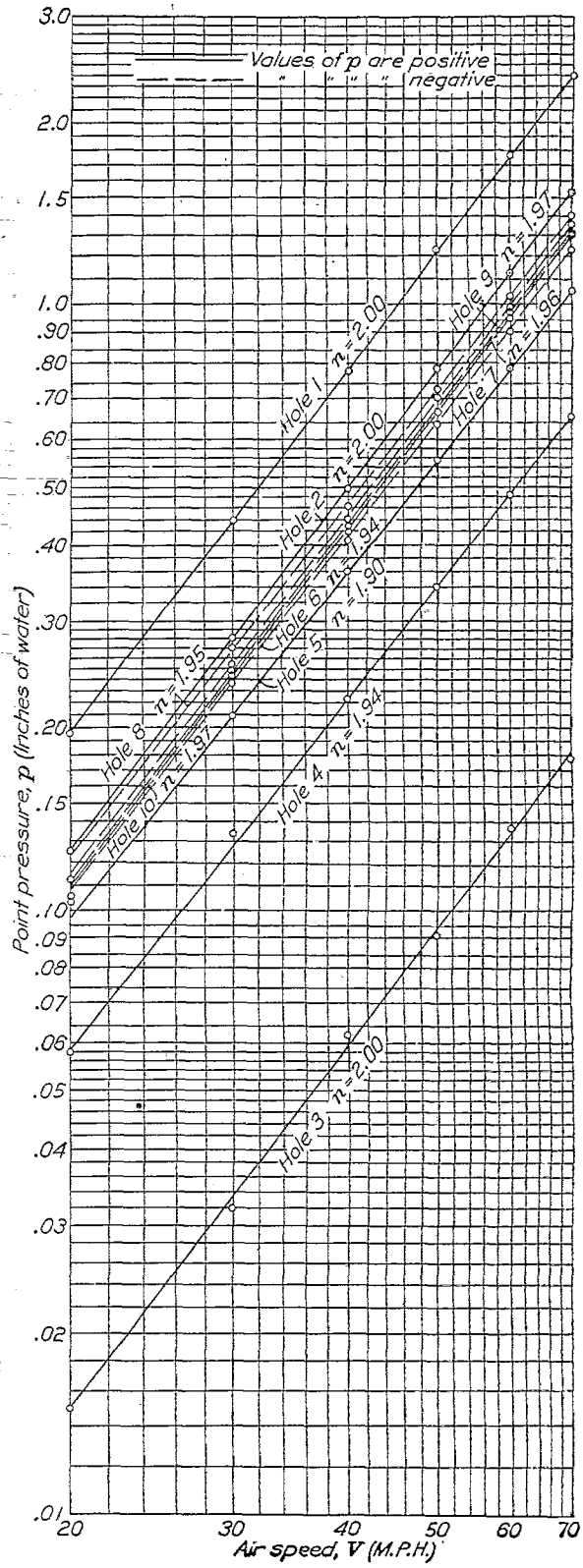

FIG. 13.—Elliptic cylinder with fineness ratio of 4. Model at 0° pitch and 0° yaw

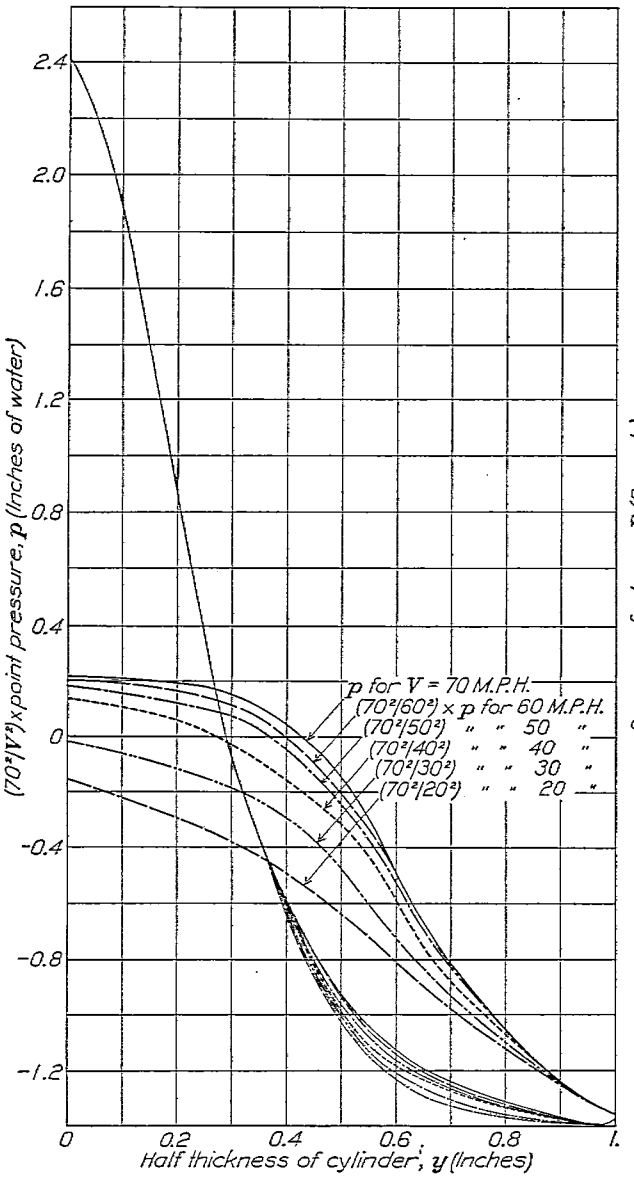

FIG. 14.—Elliptic cylinder 2 by 8 inches, model at 0° pitch and 0° yaw

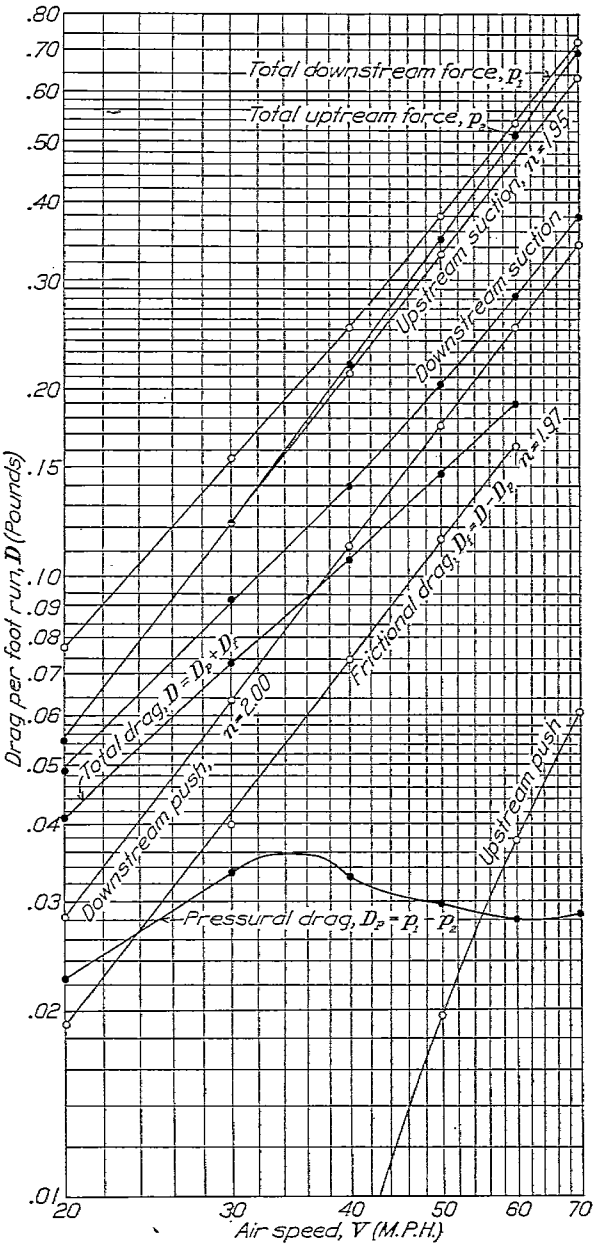

FIG. 15.—Elliptic cylinder 2 by 8 inches, model at 0° pitch and 0° yaw

Figure 16 portrays theoretical curves of point pressure and zonal pressure drag together with the measured pressure, all at 40 miles an hour, and the pressure drag computed from these measurements. Formulas for the theoretical curves are given in reference 3.

The measured pressures agree well with the theoretical except at the rear where the flow is turbulent. The pressure drag is a maximum where $p = o$ and a minimum amidships. The whole pressure drag on the front half of the model is negative. Theoretically this is balanced by the rear drag, but actually there is a downstream resultant which here is one-third the whole measured drag or one-half the friction drag.

CONCLUSIONS

From Figures 4, 6, 8, it is seen that for $V_1 d = 7.33$ (ft.$\times$ft./sec.) the best characteristics occur when the elliptic cylinder has a fineness ratio of 4.0. Figure 11 indicates that the above conclusion would hold for small Reynolds Numbers, but for large Reynolds Numbers, $V_1 d > 11$, the drag is less for a cylinder fineness ratio of 3.0 or 3.5, and this would probably result in an improved

C/D curve which would mean that improved characteristics could be obtained with a fineness ratio smaller than 4.0.

If we assume a speed of 150 miles an hour and streamline wire with a thickness of one-fourth inch, $V_1 d = 4.6$ (ft.×ft./sec.), at such a Reynolds Number an elliptic section with a fineness ratio of 4.0 would have better characteristics than a section with a smaller fineness ratio.

Comparing the point pressure over the surface of the elliptic cylinder with that over the surface of the Navy No. 1 modified strut given in Reference 4, it is seen that the maximum suction is further aft for the elliptic section, and the streamlined trailing edge of the strut results in the pressure being zero at the same point near the trailing edge for any speed, while for the elliptic cylinder as the speed decreases the pressure is zero further aft, and for the low-test speeds there is still a suction at the trailing edge. Thus the character of the air flow at the after part of the elliptic cylinder is different for different speeds.

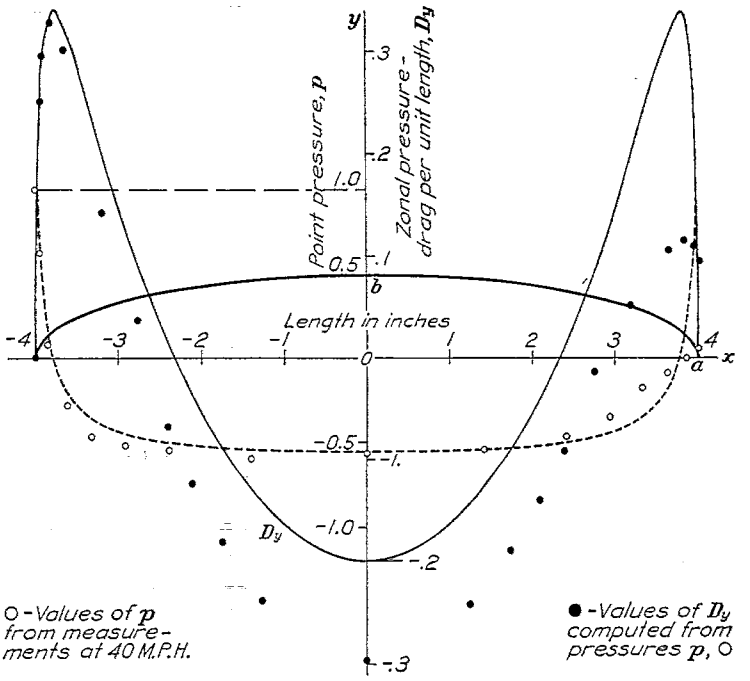

FIG. 16.—Elliptic cylinder 2 by 8 inches. Graphs indicate theoretical values. $p = 1 - (a+b)^2 y^2 / [b^4 + (a^2 - b^2) y^2]$ where unit pressure $= \rho V^2/2$. $D_y = 2 \int_0^y p \, dy$

For an elliptic cylinder or any simple quadric, fixed at any attitude in a uniform infinite stream of inviscid liquid, it can be shown, Reference 3, that the zonal pressure drag is upstream on the fore part; downstream on the rear part; zero on the whole. The model in Figure 16 exhibits these properties except that the resultant pressure drag, owing to viscosity, is not quite zero.

At 40 miles an hour the drag coefficient of the 2 by 8 inch elliptic strut, at zero yaw and with free ends, is about 2.5 times that previously found for the best Navy strut, as given in Reference 4.

REFERENCES

Reference 1.—A. F. Zahm, "The Six-Component Wind Balance." N. A. C. A. Technical Report No. 146, 1922.

Reference 2.—Aeronautics Staff, "Air Force and Center of Pressure of M-80 Airfoil." C. & R. Aeronautical Report No. 175, March 31, 1921.

Reference 3.—A. F. Zahm, "Flow and Drag Formulas for Simple Quadrics." N. A. C. A. Technical Report No. 253, 1926.

Reference 4.—A. F. Zahm, R. H. Smith, and G. C. Hill, "Point Drag and Total Drag of Navy Struts No. 1 Modified." N. A. C. A. Technical Report No. 137, 1922.

[Elliptic cylinder. Various fineness ratio]

TABLE I

SPECIFIED OFFSETS

Distance from leading edge (inches)				Thickness (inches)
2 by 5 inch cylinder	2 by 6 inch cylinder	2 by 7 inch cylinder	2 by 8 inch cylinder	
0.	0.	0.	0.	0.
.050	.060	.070	.080	.399
.125	.150	.175	.200	.624
.250	.300	.350	.400	.872
.275	.450	.525	.600	1.054
.500	.600	.700	.800	1.200
.750	.900	1.050	1.200	1.428
1.000	1.200	1.400	1.600	1.600
1.500	1.800	2.100	2.400	1.833
2.000	2.400	2.800	3.200	1.960
2.500	3.000	3.500	4.000	2.000
3.000	3.600	4.200	4.800	1.960
3.500	4.200	4.900	5.600	1.833
4.000	4.800	5.600	6.400	1.600
4.250	5.100	5.950	6.800	1.428
4.500	5.400	6.300	7.200	1.200
4.625	5.550	6.475	7.400	1.054
4.750	5.700	6.650	7.600	.872
4.875	5.850	6.825	7.800	.624
4.950	5.940	6.930	7.920	.399
5.000	6.000	7.000	8.000	0.

[Elliptic cylinder. Various fineness ratio]

TABLE II

NET MEASURED CROSS-WIND FORCE AT 30 M. P. H. AND CROSS-WIND FORCE COEFFICIENTS

Model at 0° pitch

Angle of yaw (degrees)	Cross-wind force on 62-inch cylinder C (pounds)				Cross-wind force coefficient $C_c=2C/\rho V_1^2S$ (absolute)			
	Fineness ratio							
	2.5	3.0	3.5	4.0	2.5	3.0	3.5	4.0
−6	+4.308	+4.366	+4.761	+4.969	+2.1733	+2.2026	+2.4019	+2.5068
−4	3.383	3.326	3.526	3.550	1.7067	1.6779	1.7788	1.7909
−2	1.828	+1.676	+1.741	+1.662	.9222	+.8455	+.8783	+.8385
0	+.058	−.234	−.284	−.420	+.0293	−.1181	−.1433	−.2119
+2	−1.722	−2.116	−2.344	−2.448	−.8687	−1.0675	−1.1825	−1.2350
4	−3.241	−3.698	−3.945	−4.005	−1.6350	−1.8656	−1.9902	−2.0205
6	−4.203	−4.640	−5.005	−5.247	−2.1204	−2.3408	−2.5250	−2.6470
8	−4.738	−5.353	−5.774	−6.152	−2.3903	−2.7005	−2.9129	−3.1036
10	−5.124	−5.896	−6.336	−6.886	−2.5850	−2.9745	−3.1964	−3.4739
12	−5.384	−6.146	−6.856	−7.526	−2.7162	−3.1006	−3.4588	−3.7968
14	−5.633	−6.415	−7.195	−8.037	−2.8418	−3.2363	−3.6298	−4.0546
16	−5.851	−6.645	−7.475	−8.394	−2.9518	−3.3523	−3.7710	−4.2347
18	−6.000	−6.769	−7.664	−8.489	−3.0269	−3.4149	−3.8664	−4.2826
+20	−6.109	−6.721	−7.574	−5.534	−3.0819	−3.3907	−3.8210	−2.7918

C_c = Cross-wind force coefficient = $2C/\rho V_1^2S$.
C = Net (model without holder) cross-wind force in pounds.
S = Frontal area of cylinder = 0.8611 sq. ft.
V_1 = Air speed = 44 ft./sec.
ρ = Air density = 0.002378 slug/cu. ft.

[Elliptic cylinder. Various fineness ratio]

TABLE III

NET MEASURED DRAG AT 30 M. P. H. AND DRAG COEFFICIENTS

Model at 0° pitch

Angle of yaw (degrees)	Drag of 62-inch cylinder D (pounds)				Drag coefficient $C_D=2D/\rho V_1^2S$ (absolute)			
	Fineness ratio							
	2.5	3.0	3.5	4.0	2.5	3.0	3.5	4.0
−6	0.531	0.471	0.464	0.456	0.2679	0.2376	0.2341	0.2300
−4	.501	.431	.424	.416	.2527	.2174	.2139	.2099
−2	.503	.424	.404	.385	.2538	.2139	.2038	.1942
0	.521	.441	.406	.369	.2628	.2225	.2048	.1862
+2	.507	.411	.401	.383	.2558	.2073	.2023	.1932
4	.491	.437	.411	.411	.2477	.2205	.2073	.2073
6	.501	.454	.449	.449	.2527	.2290	.2265	.2265
8	.530	.494	.498	.511	.2674	.2492	.2512	.2578
10	.566	.542	.560	.583	.2855	.2734	.2825	.2941
12	.602	.594	.628	.660	.3037	.2997	.3168	.3330
14	.643	.649	.693	.751	.3244	.3274	.3496	.3789
16	.690	.706	.756	.858	.3481	.3562	.3814	.4329
18	.736	.774	.830	.954	.3713	.3905	.4187	.4813
+20	.791	.868	.991	2.029	.3991	.4379	.4999	1.0236

C_D=Drag coefficient=$2D/\rho V_1^2S$.
D=Net (model without holder) drag in pounds.
S=Frontal area of cylinder=0.8611 sq. ft.
V_1=Air speed=44 ft./sec.
ρ=Air density=0.002378 slug/cu. ft.

[Elliptic cylinder. Various fineness ratio]

TABLE IV

NET MEASURED YAWING MOMENT ABOUT N-AXIS [1] OF MODEL HOLDER IN POUND-INCHES AT 30 M. P. H.

Model at 0° pitch

Angle of yaw (degrees)	Fineness ratio			
	2.5	3.0	3.5	4.0
−6	−2.738	−3.109	−4.587	−5.807
−4	−3.295	−3.329	−4.433	−5.135
−2	−3.821	−3.519	−3.857	−4.029
0	−3.794	−3.161	−2.727	−2.346
+2	−2.546	−1.601	−.634	+.288
4	−.640	+.522	+2.356	3.514
6	+1.404	2.856	5.444	7.092
8	3.383	5.381	8.337	10.311
10	5.244	7.860	11.528	14.406
12	7.190	10.306	14.772	18.246
14	9.218	12.376	17.856	21.828
16	11.336	14.882	20.728	25.212
18	12.963	16.837	22.633	32.251
+20	+14.696	+18.590	+24.215	+18.732

[1] N=axis is 6.91 inches above chord of cylinder for all fineness ratios, and 2.26 inches aft of nose for fineness ratio=2.0; 2.72 inches aft of nose for fineness ratio=3.0; 3.35 inches aft of nose for fineness ratio=3.5; 3.84 inches aft of nose for fineness ratio=4.0.

[Elliptic cylinder. Various fineness ratio]

TABLE V

C/D AT 30 M. P. H. FOR 62 INCH LONG CYLINDERS

Model at 0° pitch

Angle of yaw (degrees)	Fineness ratio			
	2.5	3.0	3.5	4.0
−6	+8.12	+9.28	+10.3	+10.4
−4	6.76	7.72	8.32	7.56
−2	3.63	+3.95	+4.31	+4.32
0	+.111	−.531	−.700	−1.14
+2	−3.40	−5.15	−5.85	−6.62
4	−6.61	−8.46	−9.60	−10.1
6	−8.40	−10.2	−11.4	−11.7
8	−8.94	−10.8	−11.6	−12.0
10	−9.06	−10.9	−11.3	−11.8
12	−8.95	−10.3	−10.9	−11.4
14	−8.77	−9.89	−10.4	−10.7
16	−8.48	−9.42	−9.89	−9.79
18	−8.15	−8.75	−9.23	−8.90
+20	−7.72	−7.75	−7.65	−2.73

[Elliptic cylinder. Fineness ratio=2.5 and 4.0]

TABLE VI

CROSS-WIND FORCE WITH AND WITHOUT END PLATES AT 30 M. P. H., PERCENTAGE DIFFERENCE, AND COEFFICIENT FOR INFINITE CYLINDER

Model at 0° pitch

Angle of yaw (degrees)	Cross-wind force on 62-inch cylinder (pounds)		Percentage difference $\frac{100\,(C'-C)}{C}$	Cross-wind force coefficient (absolute)	
	Without end plates C	With end plates C'		Finite cylinder $C_c=2\,C/\rho\,V_1^2S$. (See Table 2)	Infinite cylinder $C_c+C_c\times\frac{C'-C}{C}$
Fineness ratio=2.5					
−4	+3.332	+3.560	+6.8	+1.7067	+1.8228
0	−.108	−.133	23.1	+.0293	+.0361
+4	−3.226	−3.576	10.9	−1.6350	−1.8132
8	−4.801	−5.178	7.9	−2.3903	−2.5791
12	−5.591	−5.878	5.1	−2.7162	−2.8547
16	−6.155	−6.393	3.9	−2.9518	−3.0669
+20	−6.517	−6.707	+2.9	−3.0819	−3.1713
Fineness ratio=4.0					
−4	+3.376	+3.745	+10.9	+1.7909	+1.9861
0	−.070	−.078	11.4	−.2119	−.2361
+4	−3.632	−3.923	8.0	−2.0205	−2.1821
8	−6.016	−6.590	9.5	−3.1036	−3.3984
12	−7.624	−8.289	8.7	−3.7968	−4.1271
16	−8.594	−9.151	6.5	−4.2347	−4.5100
+20	−6.949	−7.796	+12.2	−2.7918	−3.1324

[Elliptic cylinder. Fineness ratio=2.5 and 4.0]

TABLE VII

DRAG WITH AND WITHOUT END PLATES AT 30 M. P. H., PERCENTAGE DIFFERENCE, AND COEFFICIENT FOR INFINITE CYLINDER

Model at 0° pitch

Angle of yaw (degrees)	Drag of 62-inch cylinder (pounds)		Percentage difference $\frac{100(D'-D)}{D}$	Drag coefficient (absolute)	
	Without end plates D	With end plates D'		Finite cylinder $C_D=2D/\rho V_1^2 S$. (See Table 3)	Infinite cylinder $C_D+C_D\times\frac{D'-D}{D}$
Fineness ratio=2.5					
−4	0 492	0. 484	−1. 63	0. 2527	0. 2511
0	. 515	. 517	+. 39	. 2628	. 2638
+4	. 498	. 494	−. 80	. 2477	. 2457
8	. 541	. 513	−5. 18	. 2674	. 2535
12	. 595	. 549	−7. 74	. 3037	. 2802
16	. 680	. 629	−7. 50	. 3481	. 3220
+20	. 798	. 758	−5. 02	. 3991	. 3791
Fineness ratio=4.0					
−4	0. 397	0. 388	−2. 27	0. 2099	0. 2051
0	. 349	. 352	+. 86	. 1862	. 1878
+4	. 389	. 379	−2. 57	. 2073	. 2020
8	. 488	. 455	−6. 77	. 2578	. 2403
12	. 641	. 577	−9. 99	. 3330	. 2997
16	. 839	. 751	−10. 49	. 4329	. 3875
+20	1. 668	1. 640	−1. 68	1. 0236	1. 0064

[Elliptic cylinder. Various fineness ratio]

TABLE VIII

DRAG AND DRAG COEFFICIENTS AT VARIOUS SPEEDS

Model at 0° pitch and 0° yaw

Air speed (M. P. H.)	Net [1] measured drag of 62-inch cylinder or 62-inch segment of infinite cylinder (pounds)	Net drag per foot run, D (pounds)	$V_1 d$ (ft.×ft./sec.)	Drag coefficient $C_D=\frac{2D}{\rho V_1^2 S}$
Fineness ratio=2.5				
20	0.316	0.061	4.88	0.3587
30	.535	.104	7.33	.2699
40	.715	.138	9.78	.2029
50	.866	.168	12.22	.1573
60	1.072	.207	14.67	.1352
Fineness ratio=3.0				
20	0.262	0.051	4.88	0.2974
30	.452	.087	7.33	.2280
40	.581	.112	9.78	.1649
50	.720	.139	12.22	.1308
60	.916	.177	14.67	.1155
Fineness ratio=3.5				
20	0.235	0.045	4.88	0.2667
30	.424	.082	7.33	.2139
40	.591	.114	9.78	.1677
50	.728	.141	12.22	.1322
60	.908	.176	14.67	.1145
Fineness ratio=4.0				
20	0.210	0.041	4.88	0.2384
30	.377	.073	7.33	.1902
40	.551	.107	9.78	.1564
50	.752	.146	12.22	.1366
60	.986	.191	14.67	.1244

V_1=Air speed in ft./sec.
d=Thickness of cylinder=0.16667 ft.
S=Frontal area per foot run of cylinder=0.16667 sq. ft.
ρ=Air density=0.002378 slug/cu. ft.

[1] Net indicates model without holder. At 0° the increment due to end effect was negligible.

[Elliptic cylinder 2 by 8 inches]

TABLE IX

OBSERVED DIFFERENCE IN PRESSURE BETWEEN NOSE AND HOLES AFT OF NOSE, dp

$$dp=\frac{1}{2}\rho V^2-p$$

Model at 0° pitch and 0° yaw

Number of hole	Air speed in miles per hour					
	20	30	40	50	60	70
	dp in inches of alcohol on 1 to 10 slope and 0.832 specific gravity					
1	0	0	0	0	0	0
2	.85	1.93	3.42	5.33	7.67	10.57
3	2.17	4.95	8.70	13.70	19.65	26.85
4	3.05	6.95	12.15	18.92	27.15	36.90
5	3.50	7.87	13.85	21.45	30.72	41.67
6	3.60	8.20	14.40	22.45	32.17	43.78
7	3.63	8.32	14.67	22.80	32.96	44.75
8	3.70	8.60	15.10	23.52	33.70	45.88
9	3.63	8.40	14.83	23.23	33.18	45.33
10	3.50	8.30	14.58	22.85	32.71	44.68
11	3.27	7.75	13.80	21.35	30.55	41.64
12	3.23	7.30	12.77	19.64	28.08	38.25
13	3.08	6.68	11.15	17.10	24.25	32.53
14	2.80	6.05	10.21	15.40	21.63	28.90
15	2.70	5.70	9.44	14.22	20.10	26.93
16	2.50	5.38	8.90	13.65	19.50	26.38
	dp converted to inches of water					
1	0	0	0	0	0	0
2	.071	.161	.284	.443	.638	.879
3	.181	.412	.724	1.139	1.634	2.233
4	.254	.578	1.010	1.573	2.258	3.069
5	.291	.654	1.152	1.784	2.556	3.464
6	.299	.682	1.197	1.866	2.674	3.640
7	.302	.692	1.220	1.895	2.741	3.721
8	.308	.716	1.255	1.955	2.803	3.815
9	.302	.698	1.233	1.932	2.759	3.770
10	.291	.690	1.212	1.900	2.720	3.715
11	.272	.645	1.148	1.775	2.540	3.462
12	.269	.616	1.062	1.632	2.335	3.181
13	.256	.556	.928	1.422	2.017	2.708
14	.233	.503	.850	1.281	1.800	2.403
15	.225	.474	.785	1.183	1.671	2.240
16	.208	.447	.740	1.135	1.621	2.194

[Elliptic cylinder 2 by 8 inches]

TABLE X

POINT PRESSURE, p, IN INCHES OF WATER AT THE 16 HOLES

$$p=\frac{1}{2}\rho V^2-dp$$

Model at 0° pitch and 0° yaw

Number of hole	Air speed in miles per hour					
	20	30	40	50	60	70
1	+0.196	+0.444	+0.786	+1.230	+1.771	+2.411
2	.125	.283	.502	.787	1.133	1.532
3	+.015	+.032	+.062	+.091	+.137	+.178
4	−.058	−.134	−.224	−.343	−.487	−.658
5	−.095	−.210	−.366	−.554	−.785	−1.053
6	−.103	−.238	−.411	−.636	−.903	−1.229
7	−.106	−.248	−.434	−.665	−.970	−1.310
8	−.112	−.272	−.469	−.725	−1.032	−1.404
9	−.106	−.254	−.447	−.702	−.988	−1.359
10	−.095	−.246	−.426	−.670	−.949	−1.304
11	−.076	−.201	−.362	−.545	−.769	−1.051
12	−.073	−.172	−.276	−.402	−.564	−.770
13	−.060	−.112	−.142	−.192	−.246	−.297
14	−.037	−.059	−.064	−.051	−.029	+.008
15	−.029	−.030	+.001	+.047	+.100	.171
16	−.012	−.003	+.046	+.095	+.150	+.217

[Elliptic cylinder 2 by 8 inches]

TABLE XI

POINT PRESSURE IN TERMS OF NOSE PRESSURE $p/\frac{1}{2}\rho V^2$, AT VARIOUS AIR SPEEDS

Model at 0° pitch and 0° yaw

Number of hole	Air speed in miles per hour					
	20	30	40	50	60	70
1	+1.000	+1.000	+1.000	+1.000	+1.000	+1.000
2	.638	.638	.639	.640	.640	.637
3	+.077	+.072	+.079	+.074	+.077	+.074
4	−.296	−.302	−.285	−.279	−.275	−.273
5	−.485	−.473	−.465	−.450	−.443	−.437
6	−.525	−.535	−.522	−.517	−.509	−.509
7	−.544	−.559	−.550	−.541	−.547	−.543
8	−.574	−.612	−.596	−.589	−.582	−.583
9	−.544	−.572	−.569	−.571	−.557	−.564
10	−.485	−.554	−.542	−.545	−.535	−.542
11	−.388	−.454	−.460	−.443	−.434	−.436
12	−.372	−.388	−.351	−.327	−.318	−.319
13	−.306	−.252	−.180	−.156	−.139	−.123
14	−.189	−.133	−.081	−.041	−.016	+.003
15	−.148	−.068	+.001	+.038	+.056	.071
16	−.061	−.007	+.059	+.077	+.085	+.090

[Elliptic cylinder 2 by 8 inches]

TABLE XII

ALONG-STREAM FORCES PER FOOT RUN OF CYLINDER EXPRESSED IN POUNDS AND IN TERMS OF TOTAL MEASURED DRAG

Model at 0° pitch and 0° yaw

Air speed (M. P. H.)	Downstream			Upstream			Pressural drag $D_p=p_1-p_2$	Frictional drag D_f	Total drag $D=D_p+D_f$
	Push	Suction	Total p_1	Push	Suction	Total p_2			
	Pounds per foot run								
20	0. 0282	0. 0490	0. 0772	0	0. 0548	0. 0548	0. 0224	0. 019	0. 041
30	. 0633	. 0921	. 1554	0	. 1222	. 1222	. 0332	. 040	. 073
40	. 1125	. 1406	. 2531	. 0068	. 2134	. 2202	. 0329	. 074	. 107
50	. 1761	. 2044	. 3805	. 0196	. 3311	. 3507	. 0298	. 116	. 146
60	. 2536	. 2855	. 5391	. 0378	. 4734	. 5112	. 0279	. 163	. 191
70	. 3450	. 3807	. 7257	. 0608	. 6363	. 6971	. 0286		
	Per cent of total measured drag								
20	69	120	189	0	134	134	55	45	100
30	87	126	213	0	167	167	46	54	100
40	105	131	236	6	199	205	31	69	100
50	121	140	261	13	227	240	21	79	100
60	133	149	282	20	248	268	14	86	100
70									

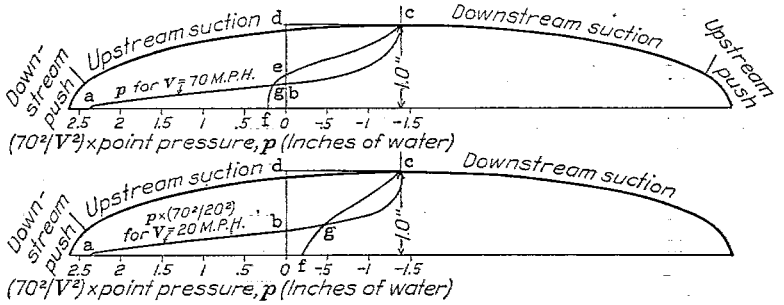

FIG. 17.—For V=40, 50, 60, or 70 M. P. H.
Downstream push ∝ abo
Downstream suction ∝ ced
Upstream push ∝ eof
Upstream suction ∝ bed
Total area=(abo+ced)−(eof+bcd)
=agf−gcg
For V=20 or 30 M. P. H.
Downstream push ∝ abo
Downstream suction ∝ cfod
Upstream push=0
Upstream suction ∝ bged
Total area=(abo+cfod)−(0+bged)
=abgf−gcg